Hydrologically Driven Slope Failure Initiation in Variably Saturated Porous Media

R.I. Borja, G. Oettl, B.A. Ebel and K. Loague

Stanford University, Stanford, USA
borja@stanford.edu

Abstract. We develop a physics-based slope failure initiation model that considers deformation and strain localization based upon three-phase continuum mixture theory for variably saturated porous media. The spatial and temporal variations in pore pressures needed to drive the slope stability model are simulated with a recently developed integrated hydrology model (InHM). To capture unsaturated soil response, the slope model has been formulated in the context of a three-phase material that explicitly accounts for the effect of the suction stress. The coupling of InHM to a rigorous slope stability model makes it possible, for the first time, to quantitatively investigate at the field-scale the nonintuitive interplay between fluid and hillslope processes that control hydrologically driven slope failure initiation.

1 Introduction

Landslides occur when earth material moves rapidly downslope after failing along a shear zone. Debris flows are differentiated from landslides by the pervasive, fluid-like deformation of the mobilized material. The formation of debris flows most often occurs as a result of a landslide partially or completely mobilizing into a debris flow. A physics-based characterization of debris flow initiation is important because of the rapid and destructive nature of these events.

A comprehensive physics-based model, known as InHM, was recently developed [5] and tested [3, 6] to simulate fully coupled near-surface hydrologic response. InHM can be employed to calculate subsurface fluid pressures in variably saturated soils. These fluid pressures can, in turn, be used to predict solid deformation and slope movement, as well as calculate several indicators of impending slope failure.

Also recently, a mechanical model for partially saturated soils has been formulated that utilizes nonlinear continuum mechanics applied to a three-phase solid–water–air material [1, 2]. This mechanical model satisfies the three master balance laws: mass, linear momentum, and energy, and, furthermore, elucidates the role of entropy inequality on the development of specific constitutive laws for a soil skeleton exhibiting nonlinear irreversible responses. The model uses an effective Cauchy stress tensor motivated by principles of thermodynamics, as well as the Cam-Clay theory of critical state soil mechanics in which the yield function depends not only on the effective stress but also on the suction stress.

The objective of this paper is to demonstrate how these recently developed hydrologic response and solid deformation models may be integrated to study the physics of hydrologically driven slope failure initiation in variably saturated porous media. The procedure consists of sequential computational modeling in which the physics-based model InHM is first used to calculate the pore pressure response, which is then supplied to the deformation model to predict the solid deformation and stress responses. The latter responses may be used to predict slope failure initiation using different stability indicators.

2 Integrated Hydrology Model

The comprehensive InHM was designed to quantitatively simulate fully coupled near-surface hydrologic response. The important and innovative characteristics of InHM include (i) adaptive temporal weighting and time stepping, (ii) robust and efficient solution methods with the solution precision and mass-balance error stipulated by convergence tolerances, (iii) solution of one system of discrete equations with spatially variable properties and boundary conditions that requires no iteration between separate surface and subsurface models and no artificial boundary conditions, and (iv) no a priori assumption of a specific hydrologic-response mechanism. InHM is capable of simulating each of the hydrologic-response mechanisms: groundwater discharge, subsurface stormflow, Horton and Dunne overland flow. Infiltration and exfiltration rates are determined in space and time by spatially variable subsurface properties, spatially and temporally variable subsurface pressure-head gradients, and spatially and temporally variable surface water depths. The flow of water in both the surface and subsurface continua is therefore intimately coupled. The governing equations are discretized in space using the control volume FE method. Each coupled system of nonlinear equations in an InHM simulation is solved implicitly using Newton iteration. Efficient and robust iterative sparse matrix methods are used to solve the large sparse Jacobian systems. Subsurface flow, in 3D variably saturated porous medium and inside macropores, is calculated by

$$\nabla \cdot f^{\mathrm{a}}\boldsymbol{q} \pm q^{\mathrm{b}} \pm q^{\mathrm{e}} = f^{\mathrm{v}} \frac{\partial \phi S_{\mathrm{w}}}{\partial t}, \tag{1}$$

where $\boldsymbol{q}$ is the Darcy flux, q^{b} is a specified rate source/sink, q^{e} is the rate of water exchange between the subsurface and surface continua, ϕ is porosity, S_{w} is degree of saturation, t is time, f^{a} is the area fraction associated with each continuum, and f^{v} is the volume fraction associated with each continuum. The Darcy flux is given by

$$\boldsymbol{q} = -k_{\mathrm{rw}} \frac{\rho_{\mathrm{w}} g}{\mu_{\mathrm{w}}} \boldsymbol{k} \cdot \nabla(\psi + z), \tag{2}$$

where k_{rw} is the relative permeability, ρ_{w} is the density of water, g is the gravitational acceleration, μ_{w} is the dynamic viscosity of water, $\boldsymbol{k}$ is the intrinsic permeability vector, z is the elevation head, and ψ is the pressure head (note, ψ is less than zero above the water table, zero at the water table, and greater than zero below the water table). The transient flow of water on the land surface (fully coupled to the subsurface) is estimated by the 2D diffusion wave approximation of the depth-integrated shallow water equations, with surface water velocities calculated with a 2D form of the Manning water depth/friction discharge equation. The subsurface fluid pressures [passed (x, y, z, t) to the slope stability model] are calculated by

$$p_{\mathrm{w}} = \rho_{\mathrm{w}} g \psi. \tag{3}$$

3 Solid Deformation Model

We consider a three-phase mixture of solid, water, and air phases and write balance of mass for each constituent as

$$\frac{\mathrm{d}\rho^{\alpha}}{\mathrm{d}t} + \rho^{\alpha} \mathrm{div}(\boldsymbol{\nu}) = -\mathrm{div}(\boldsymbol{w}^{\alpha}), \tag{4}$$

where $\mathrm{d}(\cdot)/\mathrm{d}t$ is a material time derivative following the solid phase motion, $\boldsymbol{\nu}$ is the solid phase velocity, ρ^{α} is the partial mass density of constituent α (= s, w, a for solid, water, and air, respectively), and $\boldsymbol{w}^{\alpha}$ is the Eulerian relative flow vector of the α constituent relative to the solid phase ($\boldsymbol{w}^{\mathrm{s}} = \boldsymbol{0}$, by definition).

Introducing K_{α} as the bulk modulus of the α constituent, then (1) can be re-written as

$$\frac{\mathrm{d}\phi^{\alpha}}{\mathrm{d}t} + \frac{\phi^{\alpha}}{K_{\alpha}} \frac{\mathrm{d}p_{\alpha}}{\mathrm{d}t} + \phi^{\alpha} \mathrm{div}(\boldsymbol{\nu}) = -\frac{1}{\rho_{\alpha}} \mathrm{div}(\boldsymbol{w}^{\alpha}), \tag{5}$$

where ϕ^{α} is the volume fraction, p_{α} is the intrinsic pressure, and ρ_{α} is the intrinsic mass density of the α constituent (note: $\rho^{\alpha} = \phi^{\alpha} \rho_{\alpha}$).

Balance of linear momentum for each constituent may be expressed as

$$\mathrm{div}(\boldsymbol{\sigma}^{\alpha}) + \rho^{\alpha} \boldsymbol{g} + \boldsymbol{h}^{\alpha} = \rho^{\alpha} \frac{\mathrm{d}^{\alpha} \boldsymbol{\nu}_{\alpha}}{\mathrm{d}t}, \tag{6}$$

where $\boldsymbol{\sigma}^{\alpha}$ is the partial Cauchy stress tensor, $\boldsymbol{g}$ is the gravity acceleration vector, $\boldsymbol{h}^{\alpha}$ is the volume–density force vector exerted by the other constituents on the α constituent, $\boldsymbol{\nu}_{\alpha}$ is the velocity of the α constituent, and $\mathrm{d}^{\alpha}(\cdot)/\mathrm{d}t$ is the material time derivative following the α constituent. Summing (6) for all the three constituent phases gives

$$\operatorname{div}(\boldsymbol{\sigma}) + \rho\boldsymbol{g} = \sum_{\alpha=\mathrm{s,w,a}} \rho^{\alpha} \frac{\mathrm{d}^{\alpha}\boldsymbol{\nu}_{\alpha}}{\mathrm{d}t}, \tag{7}$$

where $\boldsymbol{\sigma} = \boldsymbol{\sigma}^{\mathrm{s}} + \boldsymbol{\sigma}^{\mathrm{w}} + \boldsymbol{\sigma}^{\mathrm{a}}$ is the total Cauchy stress tensor, and $\rho = \rho^{\mathrm{s}} + \rho^{\mathrm{w}} + \rho^{\mathrm{a}}$ is the total mass density of the mixture.

Let K be the kinetic energy per unit volume and I the total internal energy per unit volume of a three-phase mixture. The first law of thermodynamics may be written as

$$\dot{K} + \dot{I} = P, \tag{8}$$

where P is the mechanical power per unit volume and the superposed dot, $\dot{(\cdot)}$, denotes a material time derivative relative to the mixture taken as a whole. Using balance of mass and balance of linear momentum, we obtain the following expression for the rate of change of internal energy:

$$\dot{I} = \sum_{\alpha=\mathrm{s,w,a}} \boldsymbol{\sigma}^{\alpha} : \boldsymbol{d}_{\alpha}, \tag{9}$$

where $\boldsymbol{d}_{\alpha}$ is the rate of deformation tensor for the α constituent. Assuming $K_{\mathrm{s}} = \inf$ (incompressible solid grains, which is a reasonable assumption for soils), (9) can be converted into the form

$$\dot{I} = \boldsymbol{\sigma}' : \boldsymbol{d} + \dot{I}', \tag{10}$$

where $\boldsymbol{d}$ is the solid rate of deformation tensor,

$$\boldsymbol{\sigma}' = \boldsymbol{\sigma} + [S_{\mathrm{r}} p_{\mathrm{w}} + (1 - S_{\mathrm{r}}) p_{\mathrm{a}}]\mathbf{1}, \tag{11}$$

is a Cauchy effective stress tensor conjugate to $\boldsymbol{d}$ and analogous to that proposed by Schrefler [4], and $\dot{I}'$ consists of additional terms not associated with the deformation of the solid phase. The effective Cauchy stress tensor $\boldsymbol{\sigma}'$ differs from the total Cauchy stress tensor $\boldsymbol{\sigma}$ by an isotropic pore pressure equal to the average of the intrinsic pore water and pore air pressures weighted according to the degree of saturation S_{r}. Thus, the total Cauchy stress tensor lends itself to the additive decomposition

$$\boldsymbol{\sigma} = \boldsymbol{\sigma}' - [S_{\mathrm{r}} p_{\mathrm{w}} + (1 - S_{\mathrm{r}}) p_{\mathrm{a}}]\mathbf{1}. \tag{12}$$

This form may be used to develop the matrix equation for the finite element problem.

4 Finite Element Model

The finite element matrix equation for the solid deformation model takes the form

$$\boldsymbol{F}_{\mathrm{INT}}(\boldsymbol{d}, \boldsymbol{p}_{\mathrm{a}}, \boldsymbol{p}_{\mathrm{w}}) = \boldsymbol{F}_{\mathrm{EXT}}, \tag{13}$$

where $\boldsymbol{F}_{\text{EXT}}$ is the nodal external force vector induced by gravity load, and $\boldsymbol{F}_{\text{INT}}$ is the internal nodal force vector induced by the solid matrix displacement vector $\boldsymbol{d}$ and the prescribed pore water and pore air pressure vectors $\boldsymbol{p}_{\text{w}}$ and $\boldsymbol{p}_{\text{a}}$, respectively. Specifically, the internal nodal force vector $\boldsymbol{F}_{\text{INT}}$ is obtained from the total Cauchy stress tensor $\{\boldsymbol{\sigma}\}$ through an equation of the form

$$\boldsymbol{F}_{\text{INT}} = \int_V \boldsymbol{B}^{\text{T}}\{\boldsymbol{\sigma}\}\,\text{d}V, \tag{14}$$

where $\boldsymbol{B}$ is the strain–displacement transformation matrix. From (12), the functional relationship $\boldsymbol{F}_{\text{INT}} = \boldsymbol{F}_{\text{INT}}(\boldsymbol{d}, \boldsymbol{p}_{\text{a}}, \boldsymbol{p}_{\text{w}})$ is evident.

Using an uncoupled solution strategy, the vectors $\boldsymbol{p}_{\text{w}}$ and $\boldsymbol{p}_{\text{a}}$ may be determined from the hydrology model (for near-surface conditions the pore air pressure is nearly atmospheric, so $\boldsymbol{p}_{\text{a}} = \boldsymbol{0}$ is typically assumed in this case). The vector $\boldsymbol{F}_{\text{EXT}}$ is constant for quasi-static loading; thus, the slope deformation response $\boldsymbol{d}$ is driven exclusively by the prescribed temporal variations of $\boldsymbol{p}_{\text{w}}$. To better elucidate the overall global algorithm, an outline of the solution is presented in Fig. 1.

Putting (13) in residual form gives

$$\boldsymbol{R}(\boldsymbol{d}) = \boldsymbol{F}_{\text{EXT}} - \boldsymbol{F}_{\text{INT}}(\boldsymbol{d}, \boldsymbol{p}_{\text{a}}, \boldsymbol{p}_{\text{w}}). \tag{15}$$

We then want to dissipate the residual nodal force vector $\boldsymbol{R}$ by finding the response vector $\bar{\boldsymbol{d}}$ at each time instant in the solution. Here we utilize Newton's method to find the roots of the nonlinear equations, and construct the

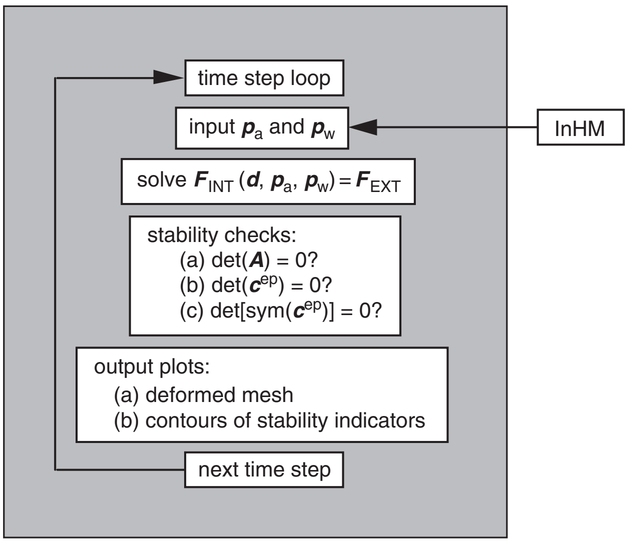

Fig. 1. Algorithm for hydrologically driven finite element deformation analysis of slopes

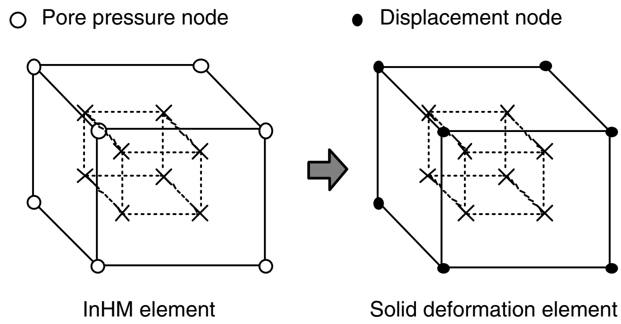

Fig. 2. Interfacing InHM with the solid deformation model

consistent tangent operator as

$$\boldsymbol{R}'(\boldsymbol{d}) = -\boldsymbol{F}'_{\mathrm{INT}}(\boldsymbol{d}, \boldsymbol{p}_{\mathrm{a}}, \boldsymbol{p}_{\mathrm{w}}) = -\partial \boldsymbol{F}_{\mathrm{INT}}/\partial \boldsymbol{d}. \tag{16}$$

Asymptotic quadratic convergence of the iterations can be expected from Newton's method provided that a consistent algorithmic tangent operator $\boldsymbol{R}'(\boldsymbol{d})$ is used.

The integrated hydrology model InHM generates spatial and temporal descriptions of calculated pore water pressures within the slope using conventional finite element approximations. Figure 2 shows a finite element used by InHM, an eight-node brick element with a trilinear interpolation of the pore water pressure field. The standard numerical integration for this element is a $2 \times 2 \times 2$-point Gauss rule in the interior of the element, denoted by the symbol $\times$. In the solid deformation model we adopt a similar level of interpolation so that the interpolated pore water pressures at the Gauss points can be used directly to evaluate the total stresses in the solid deformation model. Note that mesh locking is not engendered by the same level of interpolation for the pore water and solid displacement fields since the present approach entails an uncoupled analysis. By constraining motion in the out-of-plane direction, the brick element shown in Fig. 2 may be used for plane strain loading conditions as well.

5 Numerical Example

For preliminary numerical investigations we consider a simple example consisting of a variably saturated slope deforming in plane strain. The slope has horizontal and vertical dimensions of approximately 50 and 30 m, and is inclined at an angle of about 30°, see Fig. 3. The domain is spatially discretized using 527 constrained brick finite elements described in Sect. 4. Each element consists of nodes with horizontal and vertical displacement degrees of freedom, as well as pore water and pore air pressure degrees of freedom. The pore

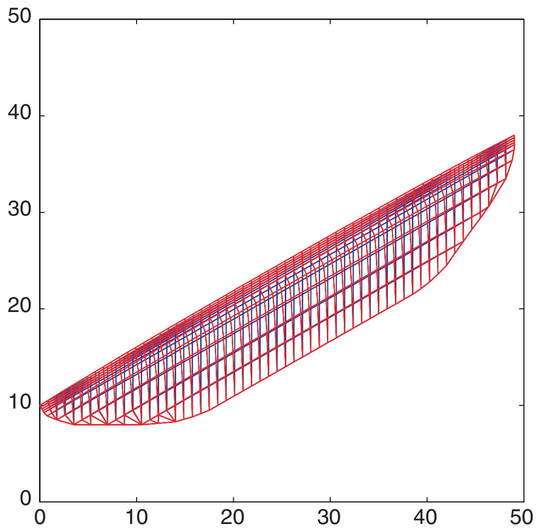

Fig. 3. Undeformed and deformed meshes (all coordinates in meters)

air pressure is assumed to remain equal to atmospheric everywhere within the slope, but the spatial distribution of the pore water pressure has been calculated by InHM and is used to drive the deformation model. For purposes of deformation analysis all nodes supporting the bottom of the slope are assumed to be pinned to the bedrock.

The soil is modeled as an elastoplastic material yielding according to the modified Cam-Clay theory and enhanced to accommodate the effect of suction on the yield condition. The mathematical framework of the constitutive model is based on a three-phase solid–water–air mixture formulation presented by Borja [1]. For the record, the material parameters used in the present analysis are the same as those used by Borja [1].

The numerical simulation of the problem consists of two steps. The first step consists of establishing the initial condition, whereas the second step consists of calculating the deformation produced by the imposed changes in the pore water pressures. The initial state is characterized by a bilinear pore water pressure distribution in the vertical direction. The ground water table marking the position of zero pore pressures is located at a depth of 2.5 m below the slope. Below the ground water level the pore water pressure increases hydrostatically; above the ground water table tensile pore water pressures (i.e., suction stresses) exist in the slope, as generated by InHM. For purposes of describing the prevailing initial yield condition, the soil is assumed to be normally consolidated everywhere.

The second step of the simulation consists of raising the ground water table elevation by about 0.9 m. This has the effect of saturating an initially unsaturated zone, as well as increasing the pore water pressures everywhere

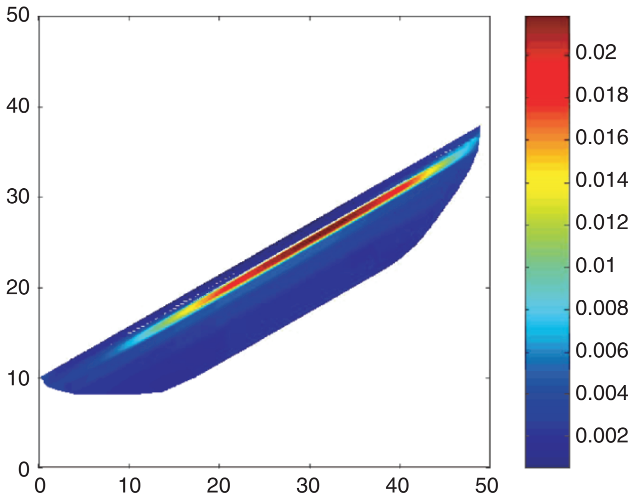

Fig. 4. Shear strain distribution (in decimals) after water table rise

in the slope. Figure 4 depicts the distribution of the shear strains in the domain after the water table rise, clearly indicating a significant shear strain concentration within a sub-region of the slope where the unsaturated zone has become saturated. This shear strain distribution agrees with a high displacement gradient forming in the vicinity of the water table rise. The vertical displacements are one order of magnitude smaller than the horizontal displacements. However, due to the imposed displacement boundary conditions where the deformations are constrained at both the top and bottom of the slope, the maximum deformations occur at about the mid-height of the slope.

6 Closure

We have developed a physics-based slope failure initiation model that considers deformation and strain localization based upon three-phase continuum mixture theory for variably saturated porous media. The spatial and temporal variations in pore pressures needed to drive the slope stability model can be simulated with a recently developed InHM. To capture unsaturated soil response, the slope model has been formulated in the context of a three-phase material that explicitly accounts for the effect of the suction stress. The coupling of a rigorous slope stability model to a hydrology model will make it possible for the first time to quantitatively investigate at the field-scale the nonintuitive interplay between fluid and hillslope processes that control hydrologically driven slope failure initiation. Work is currently in progress to apply the modeling approach to an experimental catchment that has experienced slope failure.

Acknowledgments

The first author acknowledges the support of National Science Foundation Grant No. CMS-0201317. The second author is currently supported by an Erwin-Schroedinger Fellowship provided by the Austrian Science Fund (FWF) during his visit to Stanford University. The third and fourth authors have benefited from their long and ongoing collaboration with Joel VanderKwaak and partial support from the National Science Foundation Grant No. EAR-0409133.

References

1. Borja, R.I. 2004. Cam-Clay plasticity. Part V: A mathematical framework for three-phase deformation and strain localization analyses of partially saturated porous media. *Comput. Methods Appl. Mech. Engrg.* 193, 5301–5338
2. Borja, R.I. 2006. On the mechanical energy and effective stress in saturated and unsaturated porous continua, *Int. J. Solids Struct.* 43, 1764–1786
3. Loague, K., C.S. Heppner, R.H. Abrams, J.E. VanderKwaak, A.E. Carr, and B.A. Ebel. 2005. Further testing of the Integrated Hydrology Model (InHM): Event-based simulations for a small rangeland catchment located near Chickasha, Oklahoma. *Hydrol. Process.* 19, 1373–1398
4. Schrefler, B.A. 1984. The finite element method in soil consolidation (with applications to surface subsidence), Ph.D. Thesis, University College of Swansea, C/Ph/76/84
5. VanderKwaak, J.E. 1999. Numerical simulation of flow and chemical transport in integrated surface-subsurface hydrologic systems. Ph.D. Dissertation, University of Waterloo, Waterloo, Ontario, Canada
6. VanderKwaak, J.E. and K. Loague. 2001. Hydrologic-response simulations for the R-5 catchment with a comprehensive physics-based model. *Water Resour Res* 37, 999–1013